Chapter 3

Jagged1 overexpression rescues muscle function in a week-old dystrophic zebrafish larva

INTRODUCTION

One of the most common forms of childhood muscular dystrophy is Duchenne Muscular Dystrophy (DMD). The clinical symptoms include limb weakness, frequent falls, difficulty in running, pseudohypertrophy of calf muscles, contractures, Gower's sign (use of arms to get up from the floor), etc., which become visible around 3-5 years of age. Gradually, the disease progresses to loss of ambulatory capacity, kyphoscoliosis, breathing difficulty, and heart weakness by 10-12 years of age. Approximately 20-30% of the patients also show non-progressive cognitive delay or dysfunction (Rae & O'Malley, 2016). Though medical care practices have improved the life expectancy of patients up to their forties, lung or heart failure results in untimely death (Lo Mauro and Aliverti, 2016; Birnkrant et al., 2018; Buddhe et al., 2018).

The causal gene DMD located on the Xp2.1 locus is one of the largest, with 79 exons spanning 2.4MB (Monaco et al., 1986; Hoffman et al., 1987; Tennyson et al., 1995), which gives rise to multiple transcripts and protein isoforms of dystrophin (Dp70, Dp116, Dp260, Dp427, etc.) in various tissues and developmental stages (Feener et al., 1989; Bies et al., 1992; Doorenweerd et al., 2017) from internal promoters (Blake et al., 2002; Muntoni et al., 2003). Mutations disrupting the reading frame and resulting in loss of functional dystrophin (Dp427isoform only) are associated with DMD. In comparison, mutations giving rise to partially functional Dp427 expression cause late-onset, milder forms of Becker's Muscular Dystrophy (BMD). The locus is also associated with X-linked Dilated Cardiomyopathy (XLDCM) without muscle phenotype, as mutations affect dystrophin expression only in the heart (Muntoni et al.,1993).

The Dp427 is expressed in skeletal muscle, the heart, and some brain regions as a part of membrane-associated complexes called DAPC (Dystrophin Associated Protein Complex). Dp427 is a large protein consisting of actin-binding N-terminal CH1 and CH2 domains, a hinge region followed by a string of 20-24 spectrin-like repeat domains, a cysteine-rich region, and a C terminal region that binds with β-dystroglycan of DAPC. The DAPC comprises 28-30 proteins, also called Dystroglycan Protein Complex (DGC), as most proteins are glycosylated.

The DAPC and Integrins bind to extracellular matrix components on the outside and actin cytoskeleton on the inner side to stabilize the mechanical forces generated during sarcomeric contraction, which is compromised in DMD (Campbell and Kahl., 1989; Suzuki et al., 1992; Jung et al., 1995; Ishikawa-Sakurai et al., 2004; Hnia et al., 2007). Hence, the absence of dystrophin causes higher incidences of muscle damage, membrane lesions in response to contraction, and disruption of ion balance (Mokri & Engel, 1975; Ohlendieck, 2000; Houang et al., 2018). The higher and persistent intracellular calcium further activates the cascade of proteasomal degradation (Ohlendieck, 2000), oxidative stress (Whitehead et al., 2010; Lindsay et al., 2018), as well as depresses mitochondrial ATP generation (Rbyalka et al., 2014). Though mechanical stretch-mediated activation of Nox2 containing NADPH Oxidase Complex has also been implicated in higher cytoplasmic oxidative stress (Whitehead et al., 2010), calcium and ROS forming a positive stimulatory loop might be contributing further to disease pathology (Görlach et al., 2015). Nevertheless, the initiation of primary pathology due to dystrophin absence is unclear. The additional contributors of pathology span from mitochondrial abnormality (Hughes et al., 2019), lipid accumulation (Saini-Chohan et al., 2012), higher inflammatory cytokines and immune cell infiltration (Rosenberg et al., 2015), proteasomal degradation (Bachiller et al., 2020; Kitajima et al., 2020), deregulated autophagy (De Palma et al., 2012; Fiacco et al., 2016; Stoughton et al., 2018; Krishna et al., 2021), deregulated histone deacetylase mediated epigenetic changes (Rugowska et al., 2021), to aberrant signaling pathways (Starosta & Konieczny, 2021), without clear cause-effect relations.

Steroids delay disease progression by 2-3 years and improve several aspects of a patient's condition despite side effects (Matthews et al., 2016; Marden et al., 2020). Although gene therapies have started showing functional improvement in clinical trials (Campbell et al., 2020), they are not accessible, affordable, or applicable to all patients. In addition, there are still concerns with mini-dystrophin delivery concerning an immune reaction to vectors or transgene (Mendell et al., 2010; Ramos & Chamberlain, 2015; Abdul-Razak, 2016). Hence, it is important to continue seeking therapies that can work irrespective of causal mutations.

Preclinical models like *mdx* have been beneficial for investigating molecular mechanisms of pathology in DMD (Manning & O'Malley, 2015; Swiderski & Lynch, 2021). Nevertheless, the therapies targeting pathological processes like calcium, ROS, autophagy, and Nitric Oxide, which ameliorated structural and functional aspects in *mdx,* have consistently failed in clinical trials. Several factors like small size, telomere lengths, gait, utrophin upregulation, and revertant fibers (Pigozzo et al., 2013) modify disease and therapy outcomes in *mdx* mice (Partridge et al.,

2013; Yucel et al., 2018; Gaina & Popa, 2021) which may be different in DMD patients. The Golden Retriever is a severe model of DMD (GRMD) with loss of ambulation in 3-6 months and early death at ~1-1.5 years. However, the significant problems include difficulty to maintain mutations, time-consuming and high maintenance cost (McGreevy et al., 2015). Zebrafish express components of DGC (Guyon et al., 2003; Steffen et al., 2007) and develop severe dystrophic phenotype in the absence of functional dystrophin (Bassett & Curie, 2003; Guyon et al., 2009), and because of that, it has been increasingly used to assess potential therapies. The ease of maintenance in this time and cost-effective zebrafish model comes with an additional advantage of large clutch size. Dystrophic larvae can be quickly evaluated in large numbers for better statistical analysis providing a unique opportunity for large-scale drug screening (Kawahara et al., 2011; Kawahara & Kunkel, 2013; Waugh et al., 2014; Widrick et al., 2019; Farr et al., 2020; Hightower et al., 2020; Licitra et al., 2021). Muscle birefringence is a direct measure of muscle damage, hence, used to quickly assess treatment effect in preclinical studies in 2 to 4 days post-fertilization (dpf) larvae when the pathology is just beginning. Many such drugs showing birefringence correction in zebrafish were able to rescue pathology in *mdx* (Adamo et al., 2010; Nio et al., 2017; Batra et al., 2019). However, they exacerbated patient conditions in clinical trials (Timpani et al., 2021). This necessitates more thorough preclinical studies to assess potential therapeutic agents (Grounds et al., 2008; De Luca, 2012). In addition to the model type, what should constitute a rescue in preclinical models of DMD has also been a point of contention.

A previous report showed complete rescue of DMD in the severe models of Golden Retriever and *Sapje* zebrafish larvae due to increased Jagged1 expression (Vieira et al., 2015). The "Escaper" GRMD had a single mutation in the Jagged1 enhancer region, creating a myogenin binding site that resulted in a 2-fold increase in protein expression restricted to muscles. The study also showed a 70% decrease in larval death of dystrophic zebrafish at one month when injected with Jagged1 mRNA. However, the structural and functional aspects rescued by Jagged1 in the zebrafish model of DMD have not been described till now. A study of this effect can also help decide meaningful preclinical indicators in the zebrafish model for drug screening in the future.

CRISPR/Cas9 mediated knockout of the DMD gene was carried out in the study presented here. The rescue was done by co-injecting a non-integrating plasmid containing human Jagged1 ORF. The plasmid under the CMV promoter is expected to express Jagged1 for a longer time than mRNA, though randomly. Here, we checked the effects of Jagged1 overexpression on muscle

structure and function in the zebrafish model of DMD at 4 and 8 dpf. This is the first report of the Jagged1 overexpression effect on muscle structure and function in dystrophic zebrafish.

MATERIALS AND METHODS

ETHICAL APPROVAL

The procedures followed in the study were approved by the Institutional Animal Ethics Committee (No. MSU-Z/IAEC-3/10-2019).

CRISPR/CAS9 MEDIATED KO AND OVEREXPRESSION PLASMID

The annotated zebrafish DMD gene sequence (Ensembl: ENSDARG00000008487) was used. Only exon sequences of exons 4-8 were used in CasDesigner and CHOPCHOP tools to find suitable "NGG" pam sequences. The 20-24 nucleotides preceding "NGG" were used as NCBI BLAST input, and predicted targets were confirmed. Only highly efficient guide RNAs were selected against exon 6 and 7 that did not show off-targets in CRISPR tools or NCBI BLAST. For in vitro transcription of guide RNAs, the 66 nucleotide primers were synthesized containing T7 promoter sequence and target guide RNA sequence, followed by constitutive gRNA sequence. These primers were used for first-strand synthesis, followed by PCR and invitro transcription according to the manufacturer's instructions (Abm GeneCraft-R classic sgRNA synthesis kit #G952). The pCS2-Cas9 (from *S. pyogenes*) under CMV promoter was a gift from Alex Schier (Addgene plasmid #47322; http://n2t.net/addgene:47322;RRID: Addgene_47322). The pcDNA3.1 human Jagged1 CDS plasmid with CMV promoter was a kind gift from Prof. Rajan Dighe and Prof. Annapoorni Rangarajan, IISc, Bangalore. Primers for sgRNA synthesis are given in the table 2.2 in chapter 2.

GENERATION OF DMD KNOCKOUT ZEBRAFISH

Zebrafish (*Danio rerio*) from a local aquarium was raised with the standard protocol (as described in the Zebrafish book at zfin.org.) The single-cell embryos were collected and injected with pCS2:Cas9 plasmid and a mixture of 3 guide RNAs (Table 2.2 in chapter 2) with or without pcDNA3.1-hJagged1formed DMD and DMD+Jag1 rescue groups. The final concentration of ~ 30 ng/embryo after dilution with 1:1 phenol red dye was injected till embryos reached the two-cell stage. The control larvae were injected with only phenol red dye. The Jagged1 plasmid-injected control embryos were used for comparison. The FemtoJet microinjector (Eppendorf™, Germany) and glass-pulled needles were used for injection.

GENOMIC PCR

The genomic DNA from individual 5-day-old larvae was isolated (QIAGEN DNeasy Blood & Tissue Kit # 69504). The genomic regions immediately spanning target exons (700bp) and additional bracketing -1200bp was PCR amplified with primers (for 700bp) forward "ACTGTATGTGCATCCTCTCC", reverse "TCTGTATCGCTCAGAACAG"; and (1200bp) forward "GGTCAAAACCATGCTGTCATTACT," reverse "ACCCCCAAATCGAGCATCAAC" were used respectively. The 79th exon ~327bp PCR was used as a positive control with forward "TGTCAACAACTGGACCGGA" and reverse "TGAGTTGATAAAGCACCCCTGT" primers (Figure 3.1). From every 10 hatched larvae from each group, 3 larvae were randomly selected. The entire experiment was discarded if all three selected larvae showed correct bands and sequence alignment with the control.

IMMUNOHISTOCHEMISTRY ON WHOLE LARVAL TAIL MUSCLES

Two larvae from each group in each experiment set were used for knockout confirmation by dystrophin immunolocalization in tail muscles. The 4 dpf larvae were fixed overnight in 4% PFA at 4°C, transferred to 100% methanol, and rehydrated gradually by incubating in 75%, 50%, 25% methanol, washed with PBTx (PBS with 0.3% Triton X) 5 times for 10 mins; blocked in 3% BSA for 2 hours; antibody (DMD: cloud clone; β-Dystroglycan: DSHB; cardiacMyh7β-cloud clone) in blocking overnight at 4°C; 3 times 10 min washes in PBTx, incubation in blocking buffer, followed by secondary antibody (Alexa Fluor conjugated anti-mouse, ThermoFisher), Hoechst and FITC/TRITC conjugated phalloidin (ThermoFisher, USA); 3-5 times washed in PBTx and mounted with VECTASHIELD Antifade Mounting Medium (Vector Laboratories, USA) in glass slides and imaged using either Leica SP8 confocal microscope or ZEISS Airyscan microscope at 10X, 40X and 63X as required.

BIREFRINGENCE ANALYSIS

Bipolar imaging can reveal muscle degeneration without antibodies or higher magnification confocal microscopy; hence, large larvae can be assessed quickly. The 4 dpf and 8 dpf old larvae from each group were prepared according to Nongthomba & Ramchnadran, (1999) in methyl salicylate for bipolar microscopy. The two polarizers were fixed on an upright Olympus SZX-AN microscope with Leica DFC 300 FX imager. The polarizers were rotated till the background became utterly dark. The images were analyzed with Image J software. The mean intensity of

pixels (arbitrary unit - a.u.) after conversion to 8-bit greyscale images was normalized with the area. The percent birefringence was calculated by the formula given below:

$$\% \text{ Birefringence} = (\text{Intensity} \times 100) \div \text{Maximum intensity}$$

The mean intensity, percent birefringence, area, and normalized intensity values were statistically analyzed. Initially, 4-day and 8-day groups were considered separately, but the decline in birefringence was insignificant between 4 and 8-day DMD groups. Hence, the datasets were merged.

SWIMMING ACTIVITY ASSAYS

Two swimming assays were performed on zebrafish larvae at 4 and 8 dpf ages. In the spontaneous swimming assay, the larvae were left in the center of the 100 mm Petri plate with E3 medium, and movement video was recorded for 2 mins. In Touch Evoked Escape Assay – the larvae were released in the center of a 100 mm petri dish, and a fine brush or metal loop was used to touch the larva to evoke their escape behavior. Three stimuli per minute were given as and when the larvae became stationary. The videos were converted to 10 frames/second GIF files with the Wondershare tool. The GIFs were then manually traced with the M track J plugin in Image J. The mean values of 3 such 1 min sets were used for each group of larvae. The M track J software generated data containing x and y coordinates, distance traveled between points, and angle of movements. When the angle of movement was less than ±160-180°, it was considered a sharp turn. The frequency of sharp turns was considered for calculating the group mean and SD from all the individuals in the group. The mean distance (of stride) was taken as the distance between single frames. The total distance was added to all data point distances within 1 minute. The mean stride length of more than 1.5 mm was considered an event of fast swimming. Three independent experiments were used for statistical analysis.

STATISTICAL ANALYSIS

For Birefringence – Mean intensity values, % Birefringence, and area normalized mean were calculated for individual larvae in each group to compute group Mean and SD. The mean of stride length, total length, frequency of turns, and quick swim events were counted to calculate group Mean and SD based on all individuals within the group. For birefringence and swimming assay data, Mean and SD data for three independent experiments were analyzed for two-way ANOVA with Tukey's Multiple Comparison tests using GraphPad Prism (version 7.0 for

Windows, GraphPad Software, San Diego, California, USA). A p-value less than 0.05 was considered significant. The number of larvae in a single group was more than five in all experiments. The three groups were uninjected controls, DMD, and DMD injected with Jagged1 plasmid.

RESULTS

CONFIRMATION OF DMD KNOCKOUT WITH GENOMIC PCR AND IHC OF WHOLE LARVAL TAIL MUSCLE.

Dystrophin (Dp427) is a member of DGC and known to accumulate more at myotendinous junctions. Due to the repeating pattern of muscle arrangement in the form of myoseptum in zebrafish, the boundaries are stained more prominently when antibodies against DGC proteins like dystrophin or dystroglycan are used for immunohistochemical analysis of whole larval muscles. The smaller isoforms of dystrophins have broader expression patterns within tissues and cells. Staining with c-terminal specific antibodies shows signal not accumulated at myoseptal boundary and reduced overall expression in knockout larvae (Figure 3.2A). The knockout was also confirmed by bracketed genomic PCR of the targeted region. If the target region PCR is the same as in control larvae, additional sequencing was carried out to check for smaller changes in the DMD gene, which could indicate aberrations during the NHEJ repair (Figure 3.2B-C). If IHC and PCR could not confirm the absence of dystrophin, then that experiment was discarded.

THE MEMBRANE STRUCTURE IMPROVEMENT AND NUCLEAR B-DYSTROGLYCAN LOCALIZATION RESCUED BY JAG1 OVEREXPRESSION

The β-dystroglycan binds to both the transmembrane α-dystroglycan and dystrophin in the subsarcolemmal regions. The whole muscle immunostaining of β-dystroglycan in the dystrophic larvae reveals the disrupted muscle structures, visibly improved in the Jag1 OE group (Figure 3.3). Here, the aim was to visualize membrane disarray mentioned in the myoseptum of dystrophic larvae, which is seen here as well and reduced in Jag1 rescue of DMD. The nuclear signal for β-dystroglycan was unexpected, which has not been reported in DMD. This could also be a processing artifact, which will need further validation. In addition, the Hoechst counterstain also shows altered nuclear morphology. As far as previous studies are concerned, they have shown oval nuclei in control versus rounded nuclear morphology from DMD zebrafish muscles (Bruusgaard et al., 2003; Kilroy et al., 2022). Though not quantified

here, qualitatively, the improvement in the nuclear morphology in the Jagged1 rescue can be seen compared to DMD larval muscles (Figure 3.4).

JAG1 OVEREXPRESSION IMPROVES MUSCLE BIREFRINGENCE IN DYSTROPHIC LARVAE, WHILE SLOW-TYPE MUSCLES REMAIN UNAFFECTED

The result here reveals reduced birefringence of dystrophic larvae, which is partially rescued by Jagged 1. The mean of percent birefringence for the control group (60.23±2.34) reduced in DMD (35.02±3.76), which increased in the rescue group (49.08±5.75) (Figure 3.5A, D, Table 3.3). The control group had a birefringence mean intensity value of 147.28±10.72 while DMD larvae had 74.01±15.44, which improved to 109.81±30.64 in Jagged1 injected DMD group (Figure 3.5C, D, Table 3.2). The area normalized values of mean intensity for control (13.21±4.04) reduced significantly to 4.81±2.27 in DMD as well as in DMD+Jagged1 (11.83±6.59) (Figure 3.5B, Table 3.1). When intensity values were normalized to the area, the difference between control and rescue became non-significant, suggesting complete rescue. The rescue group's variability is much higher than the control or DMD group, which can be attributed to the random distribution of the non-integrating plasmid.

The cardiac MYH7β is enriched in slow-type muscles, hence used here to visualize specifically slow muscle structure. Immunostaining on the whole larval tail muscles shows a similar structure in DMD and Control group at the 8dpf stage (Figure 3.4E). There was no noticeable difference in the Jagged1 overexpression in the dystrophic or non-dystrophic group.

JAGGED1 OVEREXPRESSION PRESERVES MUSCLE FUNCTION IN OLDER ZEBRAFISH LARVAE.

The four aspects – swim stride length, total length, frequency of turns, and frequency of quick swims- are used to assess muscle function in spontaneous activity assay (SAA) comprehensively and evoked escape assays (EEA). Speed is the most popularly used measure for muscle function in dystrophic zebrafish larvae, but manual tracking made it a less reliable measurement, and hence it was not used in the present study. The manual method also made it challenging to define freeze behavior, therefore not found fit for quantitative analysis. The graphs (Figure 3.6: A-D, Table 3.4, 3.5, 3.6, 3.7) show that only swim stride length is reduced in dystrophic larvae during the spontaneous assay, and all other aspects remain unaffected at 4 dpf. The impromptu swimming was negligible in dystrophic larvae at 8 dpf even evoked swimming was severely affected, and hence spontaneous activity was not quantified at 8 dpf. One reason is that SAA is not different from control and DMD could be due to the short

duration. For proper assessment, longer durations, like 24 hours, may be required, which is not feasible with the current methods. The very high mean stride length was usually seen at the start of the experiment when larvae released in the plate tend to swim away very fast, which is reduced in dystrophic larvae.

The evoked escape behavior is crucial for survival in zebrafish larvae. At 4 dpf, the mean stride length is the only measure affected in dystrophic larvae. The total length and frequency of quick swims or turns are not affected significantly (Figure 3.6: E-H, Table 3.8, 3.9, 3.10, 3.11).

A severe reduction in swimming capacity is seen at 8 dpf in DMD larvae. At least 8-9 larvae in each replicate from the dystrophic group were completely non-responders at 8 dpf, whereas only 2-3 larvae from all replicates were non-responders at 4 dpf. The non-responders in Jagged1 rescued group were 2-3 at 8 dpf and none at 4 dpf. The non-responders were not considered for quantification. At 8 dpf, almost all controls moved before touch, while none of the dystrophic larvae showed such sensitive escape behavior.

In addition, the mean stride length reduced in DMD (0.96±0.17 mm) compared to control (1.63±0.31mm), which increased in Jagged1 rescue (1.34±0.47mm). The total distance traveled was reduced severely in DMD (2.73±0.72 mm) from control (18.03±1.05 mm) which was partially rescued by jagged1 (7.94±2.36 mm). The frequency of turns in the control group was 9.89±0.87, in DMD 1.43±0.66, and in the rescue group 4.74±0.39. The frequency of quick swimming events was significantly low in DMD (0.5±0.36) compared to control (4.47±1.29) and slightly improved in rescue (1.90±0.56) (Figure 3.7 A-D, Table 3.12, 3.13, 3.14, 3.15).

DISCUSSION

The skeletal muscle is a complex tissue generated by various types of multinucleated myofibers protected by connective tissue layers from myofiber to the fascicle to the entire muscle. The composition of sarcomeric motor myosin ATPase speed and metabolism vary coordinately to form slow oxidative type to fast glycolytic type muscles. The protein dystrophin has hundreds of interacting proteins (NCBI co-IP data), as does the DGC complex it is associated with. Thus, its absence can dysregulate several DGC functions (Ervasti et al., 2007). Several pathological mechanisms related to DMD are studied in great molecular detail (Duan et al., 2021). However, unclear causal relations in pathological processes have hampered therapy development. The mouse model mdx also shows repeated degeneration and regeneration cycles in muscle, yet functional decline is never as severe as in patients. Extensive literature suggests that the location

of muscles in the body, the width-length of muscles, and the size of an organism also affect the susceptibility to contraction-mediated injury in the case of DMD (Partridge, 2013).

Zebrafish is a cost-effective, timesaving, severe DMD model (Guyon et al., 2009). The fast- and slow-twitch muscle fibers are expressed at this early stage of development and are anatomically segregated (Devoto et al., 1996). Most tail muscles used for larval swimming are composed of fast-glycolytic type muscles, while the slow oxidative type muscles form a thin outer layer in zebrafish (Liu et al., 2021). The higher glycolytic type fibers and more dependence during larval swimming could contribute to the severe phenotype in the zebrafish model of DMD. The result shows that slow oxidative type muscles (Figure 2E) are preserved at the 8 dpf stages in dystrophic larvae. A similar finding at 5dpf has been previously reported (Stocco et al., 2021), which correlates with the supposition of slow-type muscle preservation in DMD. The activation of calcineurin-mediated transition toward slow-type muscles has shown a rescue in the mdx model (Delacroix et al., 2018). Therapies have been directed at muscle type transition but are yet to offer functional benefits in clinical trials. Based on our study, the increase in slow oxidative type muscles is not likely to be involved in Jagged1-mediated rescue. Nevertheless, the inadequacy in this study is the lack of cross-sectioning-based quantification to validate the claim.

The muscle structure is disrupted early, around 2-4 days post-fertilization in dystrophic zebrafish larvae, which is repaired via tissue-specific stem cells (Berger et al., 2010). However, the functional decline continues. The birefringence was affected similarly from 4 to 8 days, whereas muscle function declined severely from 4 to 8 dpf in dystrophic larvae, which is preserved significantly by hJagged1 plasmid injection. This is similar to what is observed in dystrophic patients. Even when the structural pathology was improved with IGF1 treatment, the functional decline continued in dystrophic patients (Rutter et al., 2020). Alternately, Jagged1 overexpression (OE) could make dystrophic muscles less vulnerable to contraction-induced injury and subsequent degeneration. Notch signaling has been shown to regulate Desmin and Vinculin-mediated myotendinous junctions (MTJ) formation in zebrafish larvae (Pascoal et al., 2013), which can improve muscle strength to mitigate susceptibility to contraction-mediated damage.

The β-dystroglycan binds to transmembrane α-dystroglycan and dystrophin in the subsarcolemmal region. The component proteins of DAPC have been suggested to be downregulated in DMD (Ervasti et al., 1990). The β-dystroglycan staining shows membrane

disruptions in myosepta, a characteristic of DMD muscles. Corresponding with birefringence data, the disruptions are reduced with Jagged1 rescue. Another interesting observation is the nuclear signal of β-dystroglycan immunostaining, which is present in myoblast nuclei (Martínez-Vieyra et al., 2013). Studies have also suggested importin-α2/β1 and exportin1/CRM1 mediated nucleo-cytoplasmic shuttling to regulate nuclear DAG levels and excess accumulation affecting nuclear morphology and cell cycle in myocytes (Lara-Chacón et al., 2010; Vélez-Aguilera et al., 2018). It is unknown if nuclear DAG levels change in DMD or if it contributes to pathology. The regeneration in dystrophic muscles is abnormal, which leads to continued expression and activity of signaling molecules like Akt/PKB, p38MAPK, and ERK1/2, involved in regeneration for an extended time compared to control in dystrophic muscles (Peter and Crosbie, 2006; Smythe and Forewood, 2012; Brennan et al., 2021). Similarly, the nuclear DAG signal could be from newly regenerated muscles. Nevertheless, further validation will be required for this observation.

Compared to elliptical in control, the rounded nuclear morphology has been associated with dystrophic muscle in zebrafish larvae and mdx mice (Bruusgaard et al., 2003; Kilroy et al., 2022). Though not quantified here, the nuclear morphology is qualitatively better in the Jagged1 rescue group than in the DMD group. The study on dystrophic zebrafish suggested that the regeneration during intervening 5-6 dpf stages results in similar birefringence in dystrophic groups at 2-4 dpf and 8-9 dpf (Kilroy et al., 2022). Hence, the similar birefringence seen at these 4 and 8 dpf stages could be due to the combinatorial effect of slow oxidative muscle preservation and regeneration of damaged muscles.

The previous study (Kilroy et al., 2022) also showed no correlation between muscle structure and function or muscle function and life span in dystrophic zebrafish. Protein degradation is known to be at a higher level in DMD, yet its inhibition has not resulted in therapy. The IGF1 treatment, which induces protein synthesis, improving several aspects of muscle pathology in DMD patients, also failed to improve muscle function (Rutter et al., 2020). The studies found that PDE inhibitor reduces pathology early in the zebrafish model (Kawahara et al., 2011, 2014). However, clinical trials showed exacerbation in children affected with DMD (Timpani et al., 2015). Another screen for natural compounds has also been found to be a disconnect between structural rescue at 8 dpf and functional recovery at 5 dpf (Licitra et al., 2021). The use of resveratrol improved the birefringence of dystrophic larvae at 8 dpf without functional improvement (Licitra et al., 2021). In contrast, the natural compound Gingerol from Ginger was found to improve swimming ability without structural improvement or changes in

mitochondrial metabolism. The same study also reported exacerbation of pathology in *Sapje* larvae with idebenone – which shows positive results in phase 3 clinical trials for protecting lung function in DMD patients (Mayer et al., 2017).

Though the automatic behavior monitoring system might be better suited than the simple Image J-based manual method used here, it is much cheaper and more convenient to assess functional rescue. In addition to the total distance and velocity of evoked escape behavior, the sharp turns and length of a single swim stroke were quantified here. The latter two swimming behaviors require much more complex coordination. However, they provide an additional measure of muscle function. The functional muscle decline is at 4 dpf but not acute, which could quickly be rescued and, therefore, may not be clinically relevant to DMD patients. The structural pathology in dystrophic muscles deteriorated at a slower rate due to intervening muscle regeneration. However, the swimming ability declined severely from 4 to 8 dpf. Despite the dilution and degradation of the non-integrating plasmid used here, the partial rescue of muscle function was evident at 8 dpf. The preclinical studies in dystrophic zebrafish do not commonly include functional recovery at 8dpf, which would be a better indicator.

CONCLUSION

The relationship between muscle structure and function, as well as muscle function and survival are complicated in DMD. The dystrophic progression also varies with muscle type, muscle location in the body, and a model organism-dependent manner. The slow-type muscles in DMD larvae at 8 days post-fertilization remained qualitatively unaffected. The functional decline from 4 to 8 dpf old dystrophic larvae is more reminiscent of disease progression than muscle structure assessed with birefringence. Though birefringence analysis is suitable for the initial large-scale screening of drugs, the functional rescue at 8-10 dpf might be a better indicator of rescue in the zebrafish model of DMD. Improved indicators for testing preclinical models, including zebrafish, should be considered to better predict the potential of the therapy at reduced risk of disease exacerbation to dystrophic children participating in clinical trials.

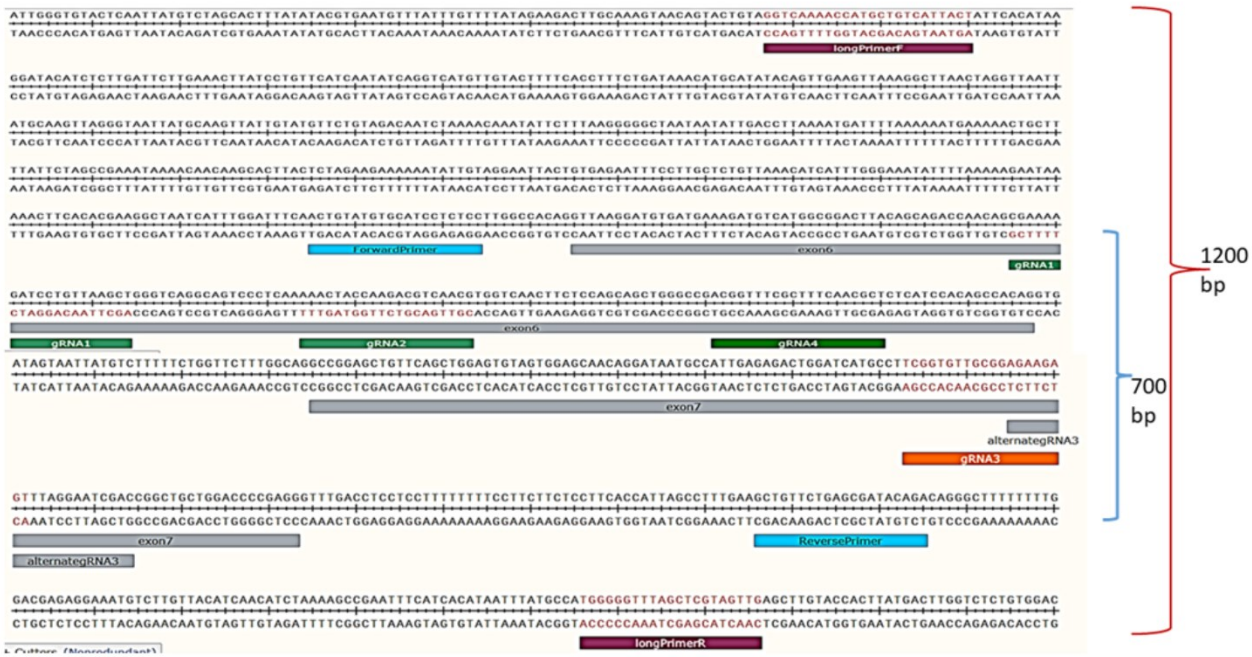

Figure 3.1: The targeted genomic region of DMD in zebrafish showing guideRNA highlighted in dark green, exons 6 and 7 regions highlighted in grey, genomic PCR primers that would generate 700 bp product in light blue and bracketing longer 1200 bp product generating primers in magenta. Image made in the Snapgene tool.

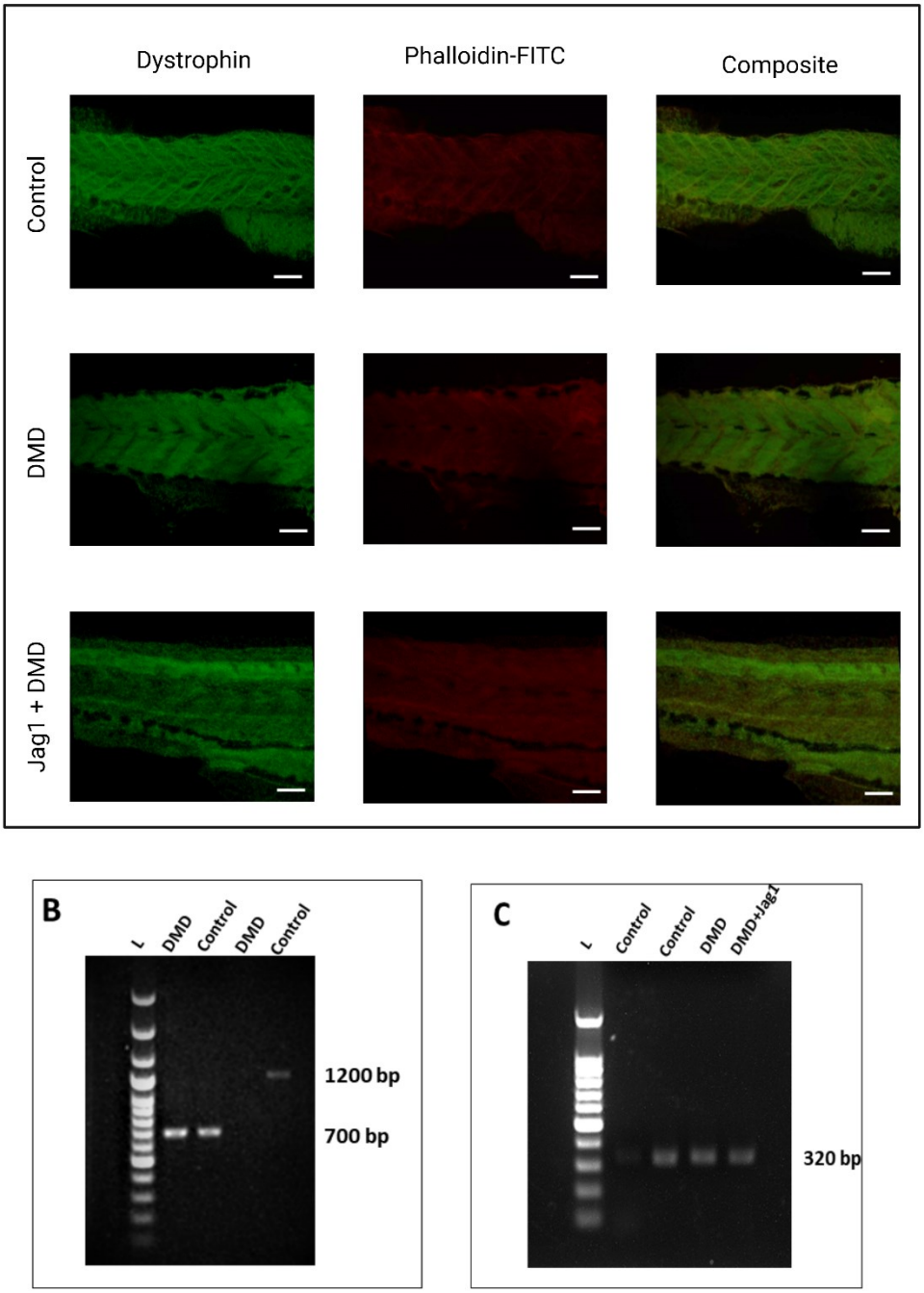

Figure 3.2: The dystrophin KO with the help of CRISPR/Cas9: A: The c-terminal dystrophin antibody staining in 4 dpf whole larval tail muscles show absence of full-length dystrophin accumulation at myoseptum in DMD and DMD+ Jag1 groups as compared to control (scale:50um); B: The genomic PCR around target area of knockout

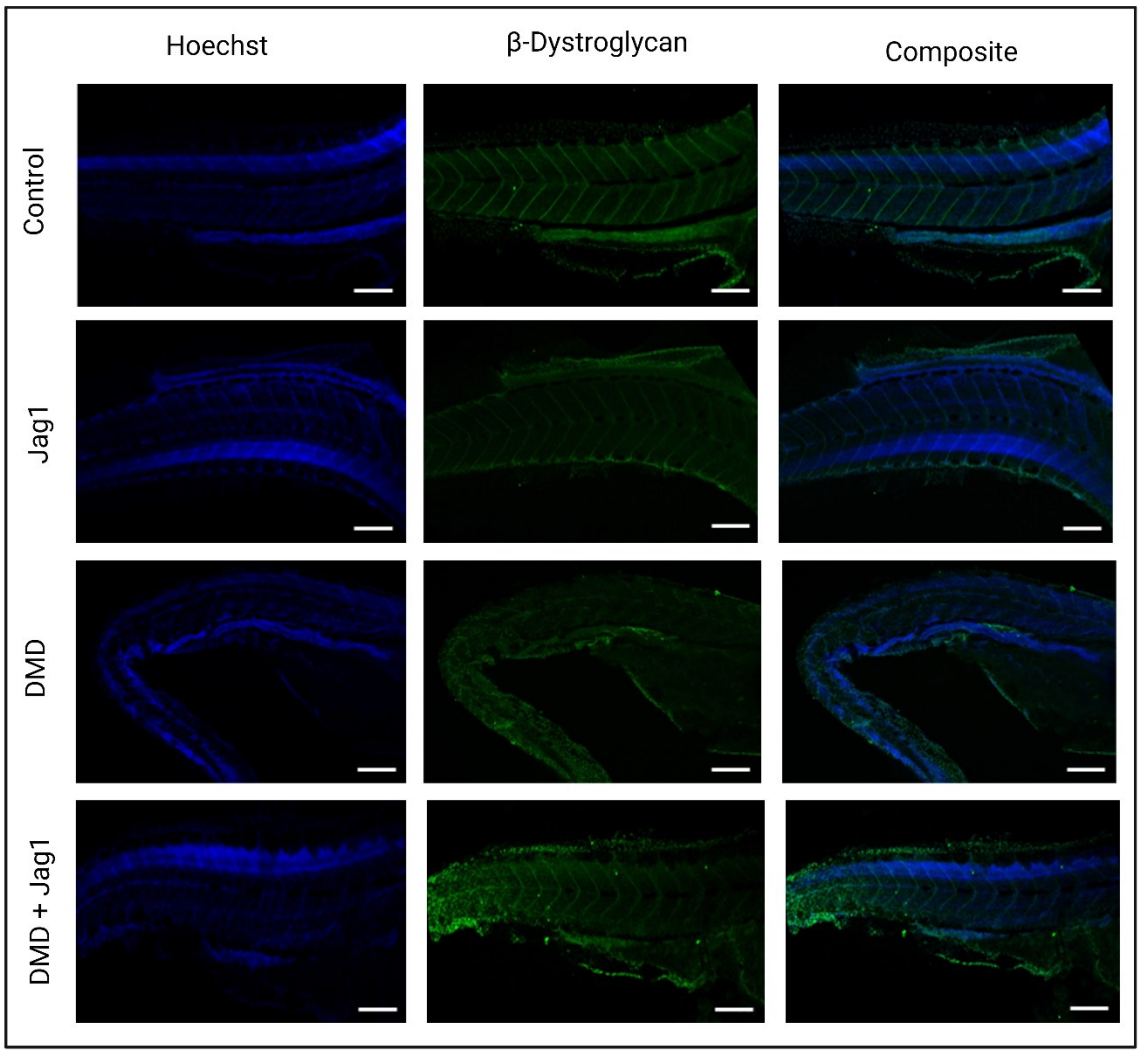

Figure 3.3: The myospetum structure disrupted in DMD is rescued by Jagged1: the confocal image of whole larval tail muscle (200um) stained for β-Dystroglycan shows disruption of structure in myoseptum in DMD KO, improvement with Jagged1 in rescue group.

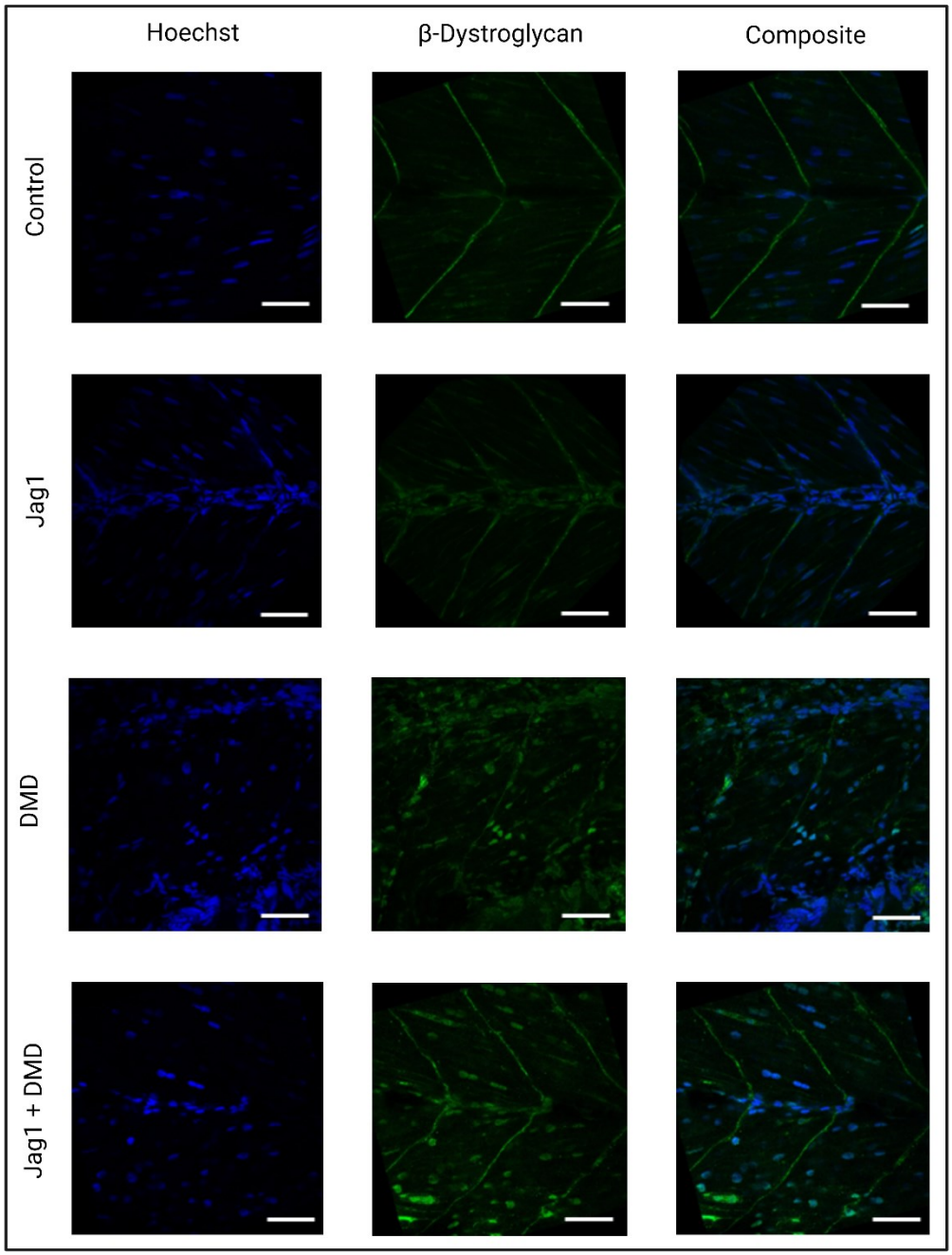

Figure 3.4: The membrane disruptions are evident in dystrophic condition, better in Jagged1 overexpression: β-dystroglycan staining (green) and Hoechst counterstaining nuclei (blue) in 8dpf control, DMD, DMD+Jag1, control+Jag1 groups (scale: 100um).

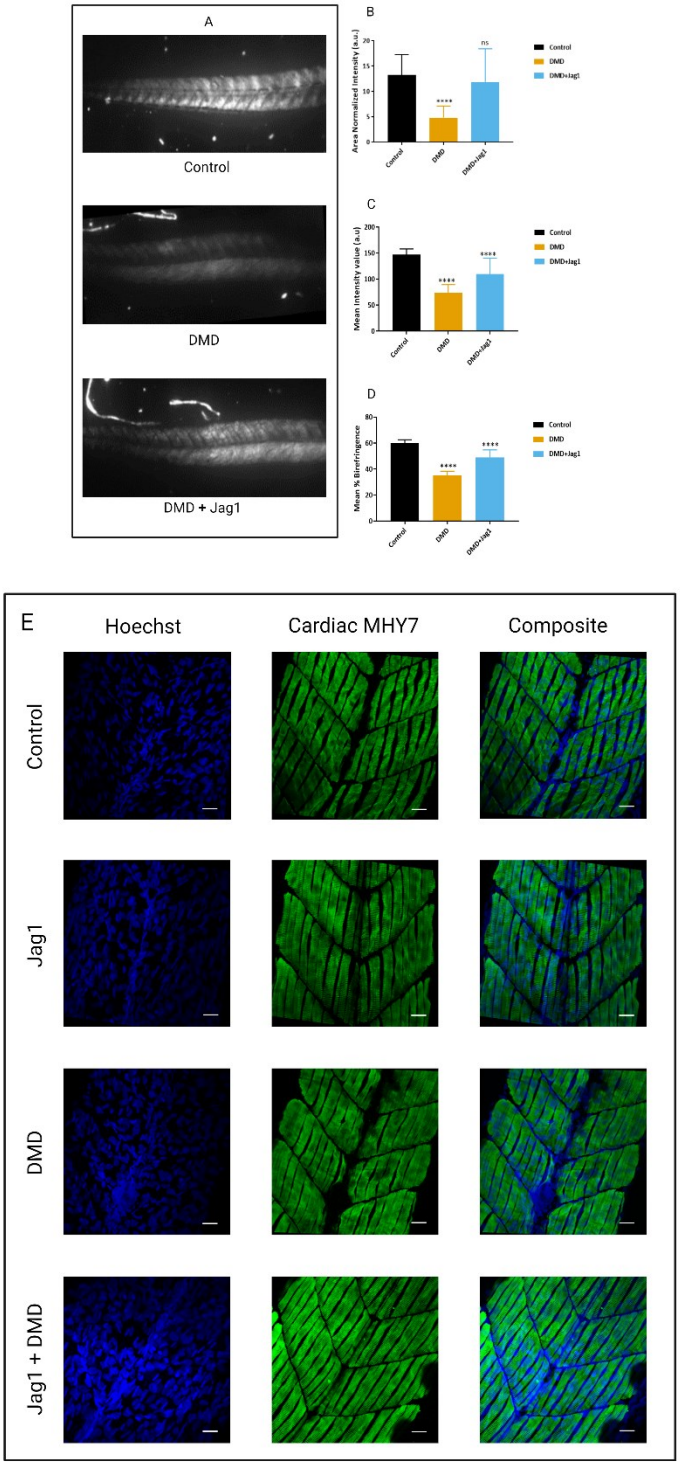

Figure 3.5: The muscle structural changes in DMD larvae are independent of slow-type muscle loss: A: representative bipolar images of whole larval tail; B: Graph comparing area normalized grey intensity (a.u.); C: Mean Intensity value (a.u.); D: mean % Birefringence between control, DMD KO, DMD KO + Jag1rescue (N=59); E: cardiac MHY7β staining of slow muscles at 8dpf stage in control, DMD KO, DMD KO + Jag1rescue show no major disruptions between groups.

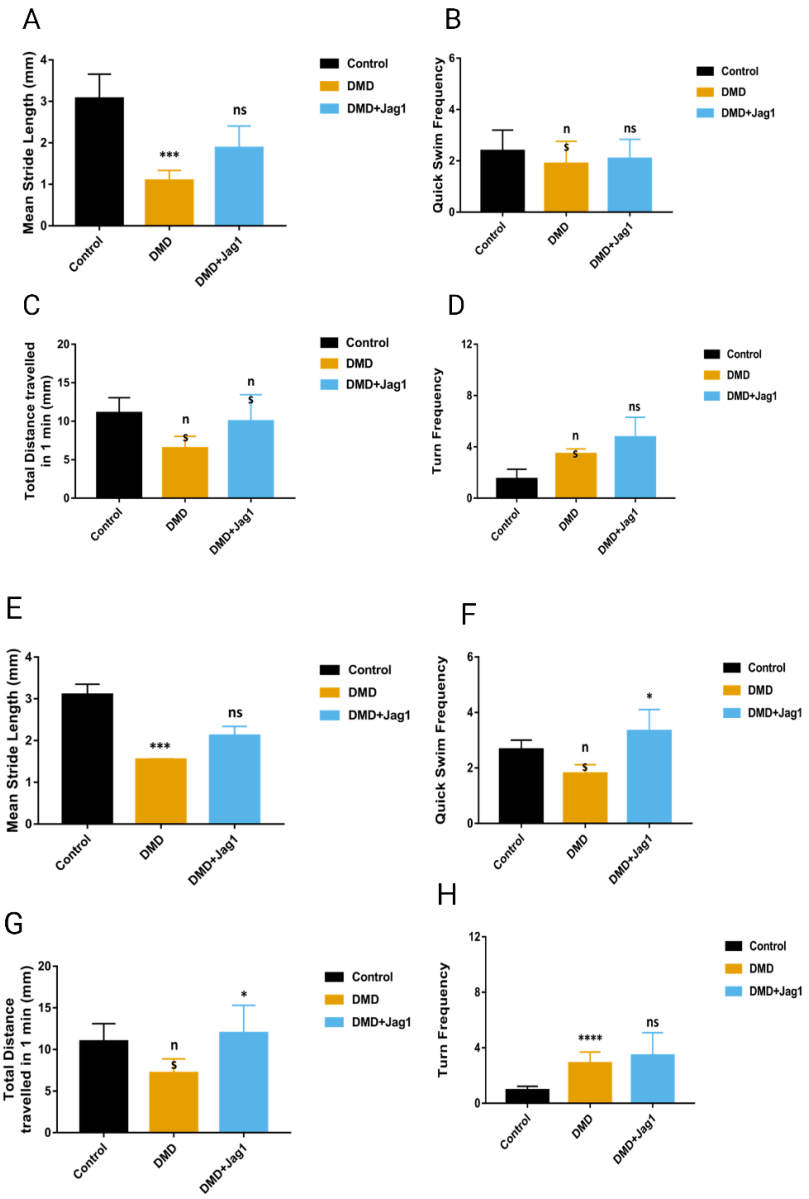

Figure 3.6: The DMD larvae show reduced swimming capacity at 4day which is rescued by Jagged1 overexpression: (A-D) Spontaneous Activity in 4 dpf old DMD KO, DMD KO + Jag1rescue (N=29); A: Mean Stride Length (mm); B: Quick swim frequency; C: Total Distance Travelled in a minute; D: Turn Frequency. (E-H) Evoked Escape in 4 dpf old DMD KO, DMD KO + Jag1rescue (N=29); E: Mean Stride Length (mm); F: Quick swim frequency; G: Total Distance Travelled in a minute; H: Turn Frequency (significance: * p< .05, ** p<.01, *** p<.001).

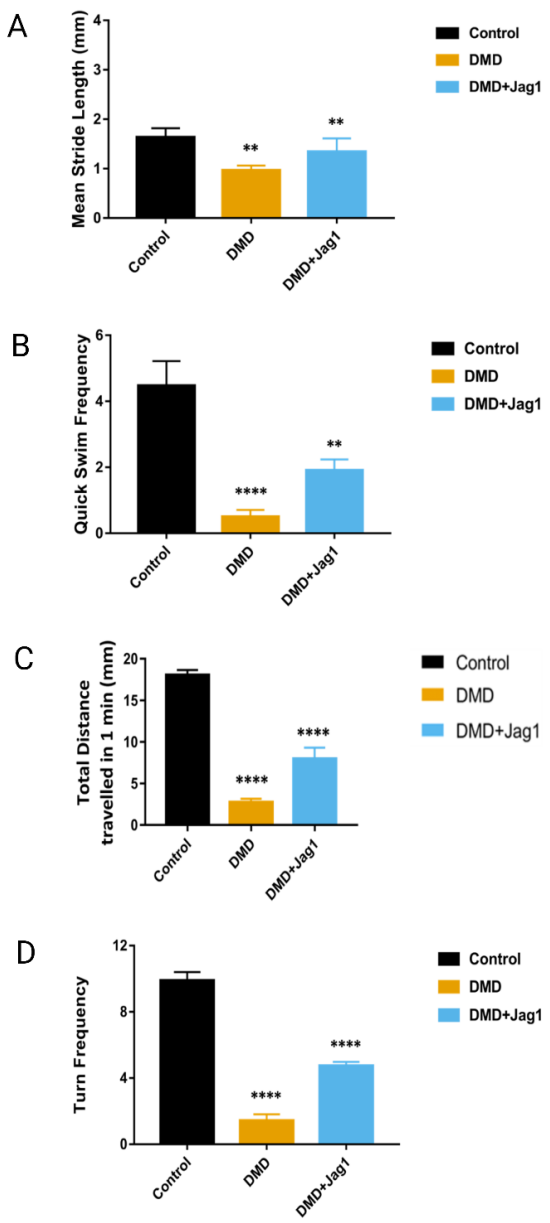

Figure 3.7: The Jagged1 overexpression rescues swimming capacity at 8 days post fertilization: Evoked Escape in 8 dpf old DMD KO, DMD KO + Jag1rescue (N=118), A: Mean Stride Length (mm); B: Quick swim frequency; C: Total Distance Travelled in a minute; D: Turn Frequency (significance: * p< .05, ** p<.01, *** p<.001).

Table 3.1: Quantification of the area normalized birefringence for larval muscle tissue.

Group	**Area normalized values of mean intensity (a.u.)**
Control	13.21±4.04
DMD	4.81±2.27
DMD+Jagged1	11.83±6.59

Table 3.2: The mean birefringence intensity values of larval muscle tissue.

Group	**Birefringence mean intensity (a.u.)**
Control	147.28±10.72
DMD	74.01±15.44
DMD+Jagged1	109.81±30.64

Table 3.3: Percent birefringence values of larval muscle tissue.

Group	**% Birefringence**
Control	60.23±2.34
DMD	35.02±3.76
DMD+Jagged1	49.08±5.75

Table 3.4: The mean of stride length of larval Spontaneous Activity Assay at 4dpf

Group	**Mean Stride Length (mm)**
Control	3.069±1.01
DMD	1.092±0.42
DMD+ Jagged1	1.879±0.91

Table 3.5: The mean frequencies of quick swimming Spontaneous Activity Assay at 4dpf

Group	**Frequency of Quick Swimming**
Control	2.389±1.39
DMD	1.889±1.50
DMD+ Jagged1	2.083±1.31

Table 3.6: The mean of total distance covered by larva Spontaneous Activity Assay at 4dpf

Group	**Total Distance Travelled (mm)**
Control	11.07±3.43
DMD	6.504±2.65
DMD + Jagged1	9.993±6.00

Table 3.7: The mean frequencies of turns exhibited by larva Spontaneous Activity Assay at 4dpf

Group	**Frequency of Turns**
Control	1.5±1.32
DMD	3.444±0.69
DMD+ Jagged1	4.75±2.70

Table 3.8: The mean of stride length of larval Touch Evoked Escape Assay at 4dpf

Group	**Mean Stride Length (mm)**
Control	3.103±0.43
DMD	1.544±0.032
DMD+ Jagged1	2.12±0.38

Table 3.9: The mean frequencies of quick swimming in Touch Evoked Escape Assay at 4dpf

Group	**Frequency of Quick Swimming**
Control	2.66±0.577
DMD	1.8±0.545
DMD + Jagged1	3.33±1.33

Table 3.10: The mean of total distance covered by larva Touch Evoked Escape Assay at 4dpf

Group	**Total Distance Travelled (mm)**
Control	10.97±3.72
DMD	7.173±2.956
DMD + Jagged1	11.98±5.767

Table 3.11: The mean frequencies of turns exhibited by larva in Touch Evoked Escape Assay at 4dpf.

Group	**Frequency of Turns**
Control	0.944±0.481
DMD	2.889±1.38
DMD + Jagged1	3.44±2.835

Table 3.12: The mean of stride length of larva Touch Evoked Escape Assay at 8 dpf.

Group	**Mean Stride Length (mm)**
Control	1.63±0.31
DMD	0.96±0.17
DMD+ Jagged1	1.34±0.47

Table 3.13: The mean frequencies of quick swimming exhibited by larva in Touch Evoked Escape Assay at 8 dpf.

Group	**Frequency of Quick Swimming**
Control	4.47±1.29
DMD	0.5±0.36
DMD + Jagged1	1.90±0.56

Table 3.14: The mean of total distance covered by larva in Touch Evoked Escape Assay at 8 dpf.

Group	**Total Distance Travelled (mm)**
Control	18.03±1.05
DMD	2.73±0.72
DMD + Jagged1	7.94±2.36

Table 3.15: The mean frequencies of turns exhibited by larva in Touch Evoked Escape Assay at 8 dpf.

Group	**Frequency of Turns**
Control	9.89±0.87
DMD	1.43±0.66
DMD + Jagged1	4.74±0.39